TEORIJSKA I PRIMENJENA MEHANIKA 15, pp 127–137, 1989, UDK 624.131.439

GREEN'S FUNCTION FOR A LAYERED HALF-SPACE WITH TIME HARMONIC LOADS ALONG ITS BOUNDARY

A. Umek and A. Štrukelj

(Received 19.10.1989)

1. Introduction. It appears that for soil-structure interaction problems forthcoming in earthquake engineering and at dynamically loaded machine foundations a homogeneous half-space model for the earth is too simplifying. To obtain a more realistic one it has to be endowed with some inner structure, which parallels that of the real earth. This however substantially increases the mathematical complexity of the problem under consideration. In our work we are trying to cope with both problems simultaneously. So a layered half-space (Figure 1) has been chosen as the physical model of the earth. The interfaces of the layers are parallel to each other and bounded perfectly to one another. The material properties inside each layer can vary from one layer to another in any way. The assumed geometry of the model can be justified by the smallness of the typical foundation dimension relative to the radius of the earth and by the fact that the layers with different material properties are almost horizontal in many practical situations. The assumption that the soil material is elastic can be justified by low power transmission per unit area of the interface between a foundation and the soil. The material damping in the soil is modeled in the case of the harmonic time dependence by the imaginary component of the elastic constants [1]. A similar physical model has been employed also by other researchers e.g. Kausel [2], Petyt and Jones [3] and others.

It appears that the dynamic properties of the layered half-space, when it is studied alone or as a substructure to a more complex problem, are most suitably given in the frequency domain and by its Green's function in space. The method of its derivation and its characteristics are the subject of this paper. We limit our attention however to the antiplane problem alone, where the only nonvanishing component of the displacement vector is directed along the z axis and is a function of x and y but not of z. It is governed by a scalar wave equation [4]. The components of the displacement vector in the plane problem and three dimensional one can be deduced from two and three potentials respectively, which also satisfy scalar wave equations as shown by Umek and Štrukelj [5]. Therefore the methods developed in this paper can be applied to solve these problems, too, however the numerical effort increases correspondingly. The other limitation we have set ourselves for this paper is that we are looking here for the Green's function for the surface

loads only, which leads to the solution of the soil-structure interaction problems for surface mounted foundations. The papers on the volume load Green's function and the corresponding embedded foundation problem are in preparation.

2. Mathematical model. The displacements inside each layer and in the underlying half-space (Figure 1) are for the antiplane motion harmonic in time, governed by a reduced scalar wave equation:

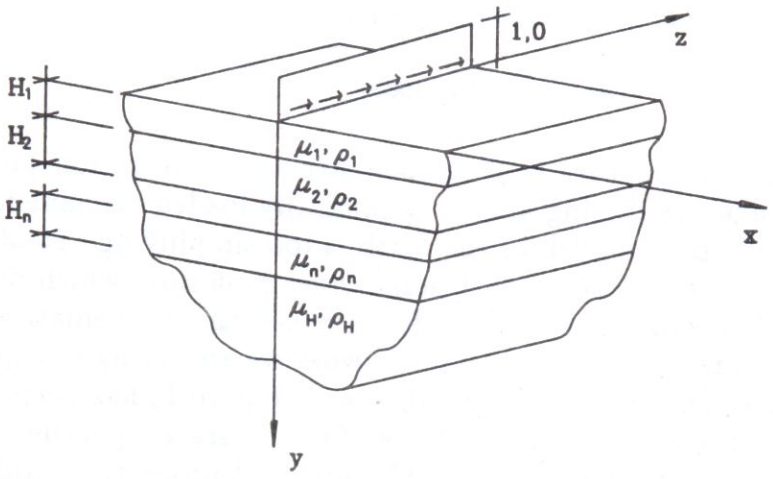

Fig. 1. The Layered Half-Space; Geometry and Material Properties.

$$c_{si}^2 \nabla^2 w_i + \omega^2 w_i = 0; \qquad i = 1, 2, \ldots, n, H \tag{1}$$

where c_{si} is the shear wave velocity and w_i the z component of the displacement vector in the i-th layer respectively and ω the driving angular velocity. It is required that the surface of the half-space is stress free, except along the z axis where a unit line load acting in the z direction is applied. Thus we obtain the following boundary condition on $y = 0$ plane:

$$\tau_{yz}(x, y = 0) = \mu_1 \frac{\partial w_1}{\partial y}\bigg|_{y=0} = -\delta(x) \tag{2}$$

where τ_{yz} is the only nonvanishing component of the stress tensor and μ_1 the shear modulus in the first layer. The perfect bonding of one layer to another and the n-th layer to the underlying half space implies the continuity of the stresses and displacements along their interfaces. This can be mathematically expressed as

$$w_i(x, y = H_i) = w_{i+1}(x, y = 0) \qquad \mu_1 \frac{\partial w_i}{\partial y}\bigg|_{y=H_i} = \mu_{i+1} \frac{\partial w_{i+1}}{\partial y}\bigg|_{y=0}. \tag{3}$$

It is required by the eliptic character of partial differential equation (1) that the boundary condition is given along a closed contour. On the other hand the semi

infinite character of the half-space implies that no boundary exists for $y > 0$ and therefore no closed contour can be drawn around it. In this case the boundary condition along the "missing part of the boundary" must be replaced by Sommerfeld radiation condition, which states that at large distances from the source only outgoing waves are present and their amplitude decays according to the law of the geometrical spreading. Its general mathematical form is given e.g. by Achenbach [4]. In our work the radiation condition is going to be satisfied after a general solution of equation (1) is derived by dropping the terms, which do not obey the above stated requirements. The mathematical form of the problem under consideration is thus given by Equations (1), (2) and (3) and the radiation condition.

3. Method of Solution. The geometry of the problem under consideration suggests that the solution could be easier derived, if the Fourier transform in the x-coordinate is introduced as:

$$W_i(\xi, y) = \int_{-\infty}^{\infty} w_i(x, y) e^{i\xi x}\, dx. \tag{4}$$

The partial differential equations (1) become in the Fourier domain ordinary differential equations, of which the solutions are:

$$W_i(\xi, y) = C_{i1}(\xi) e^{\gamma_i y} + C_{i2}(\xi) e^{-\gamma_i y} \tag{5}$$

where C_{ij} are integration constants, which are to be determined by the boundary, continuity and radiation conditions respectively and γ_i, are:

$$\gamma_i = \sqrt{\xi^2 - \omega^2/c_{si}^2}. \tag{6}$$

It can be seen that the solutions Equation (5) are from the mathematical point of view not unique, as one should expect for the motions in a linear mechanical problem, due to the square root appearing in γ_i. The uniqueness of the solutions is achieved by the introduction of the branch cuts. They can be led with respect to the layers arbitrarily, where attention shoud be paid only that the inversion path does not become too complicated. The situation in the underlying half-space is entirely different. Here the branch cuts are to be introduced in such a way that by dropping one of the terms in Equation (5) the radiation condition is satisfied, too, which implies that the real part of the γ_H must be either positive or negative in the whole complex ξ-plane. We start our derivation of the conditions for such a branch cut from the wave equation with a certain amount of damping. The assumed time dependence $e^{i\omega t}$ leads us to the reduced wave equation in the form:

$$c_{sH}^2 \nabla^2 w_H + (\omega^2 - i\omega\zeta c_{sH}^2) w_H = 0 \tag{7}$$

where ζ is the assumed damping coefficient, thus a positive real number. The further development, which parallels that given above for the undamped case, leads us to the γ_H, in which damping is included as:

$$\gamma_H = \sqrt{\xi^2 - (\omega^2/c_{sH}^2) + i\omega\zeta}. \tag{8}$$

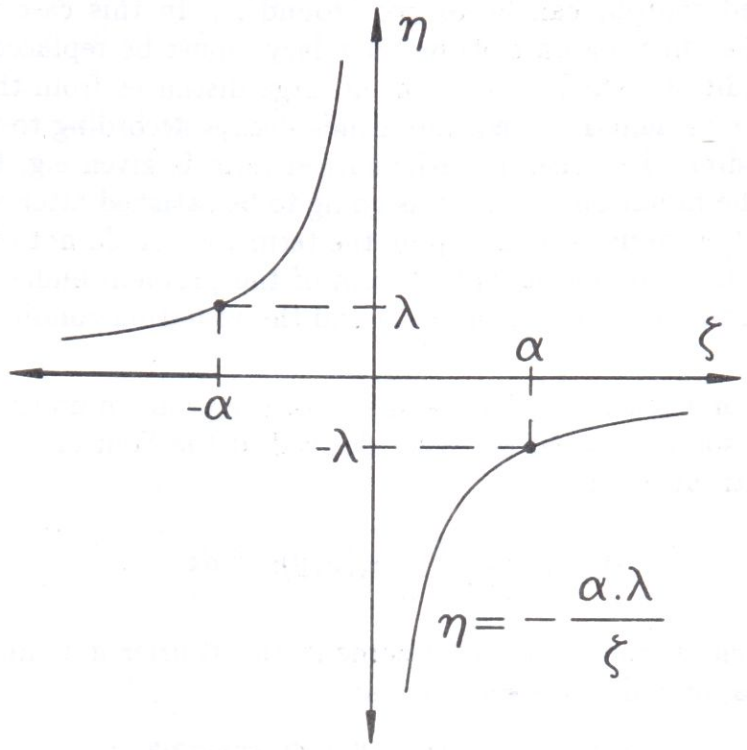

Fig. 2. Branch Points and the Corresponding Branch Cuts.

The above expression will remain positive or negative in the whole complex ξ-plane, if the phase angle of the radicand varies between $-\pi$ and π or π and 3π respectively. Therefore the imaginary part of the integrand must be zero on the branch cut. This condition yields the hyperbolas shown in Figure 2. As the branch cuts for the damped case we are free to take the inner or outer part of the hyperbolas emanating from the branch points. Taking into account the integration path of the future Fourier inverse transform it appears to be more convenient to adopt the outer portions of the hyperbolas as the branch cuts, that in the undamped case become portions of the real ξ axis from the branch points outward. The real part of the γ_H becomes in this way negative and the solution of Equation (1) for the half space, which satisfies the radiation condition, becomes:

$$W_H(\xi, y) = C_{H1}(\xi)e^{\gamma_H y}. \tag{9}$$

For reason of convenience the branch cuts for the layers are led in the same way as the ones for the underlying half-space.

The branch cuts introduced in the described way have made Equations (5) unique and have led us to the satisfaction of the radiation condition. To complete the solution in the Fourier domain these equations must be introduced into the boundary condition Equation (2) and into the continuity conditions Equations (3). As a result we obtain a system of linear algebraic equations with the integration constants $C_{ij}(\xi)$ as unknowns. It is most convenient to solve it for a limited number of layers by a computer package for symbolic algebra calculations. In our work the

program MUSIMP has been successfully applied for the casses with up to four layers, which is enough to cover most of the practical situations. In the case when more layers have to be considered the numerical solution of the equation system is the only possibility. After the integration constants are determined one or the other way, they are introduced into Equations (5), which now yield the displacement in the i-th layer in the Fourier domain. The displacement in the first layer of the one layer half-space is e.g. given by:

$$W_1(\xi, y) = \frac{\cosh[(H_1 - y)\gamma_1] - \frac{\mu_H \gamma_H}{\mu_1 \gamma_1} \sinh[(H_1 - y)\gamma_1]}{\mu_1 \gamma_1 \left[\sinh(\gamma_1 H_1) - \frac{\mu_H \gamma_H}{\mu_1 \gamma_1} \cosh(\gamma_1 H_1)\right]}. \tag{10}$$

4. Inverse Fourier's Transform. The displacement in the layers and in the underlying half-space in the Fourier domain, obtained as described in the previous paragraph must be now transformed back into the geometrical domain by the well known formula:

$$w_i(x, y) = \frac{1}{2\pi} \int_{-\infty}^{\infty} W_i(\xi, y) e^{-i\xi x} \, d\xi. \tag{11}$$

It appears that two different situations exist: the first one when the displacements can be given by an analytical formula as it is in the case e.g. of the one layer half-space problem Equation (10) and the second one in multi layer problems where the displacements due to the numerical solution of the equation system with integration constants C_{ij} as unknowns are known for discrete values of the Fourier parameter ξ only. In the latter situation it is obvious that only a numerical evaluation of the integral in Equation (11) can be performed. The detailed study of Equation (10) as the most simple case of the layered half-space problems, where the displacements can be given by an analytical formula, has convinced us that in this case too, only the numerical Fourier inversion can be introduced.

The expected difficulties with the numerical evaluation of the integral such as in Equation (11) are due to several causes: the integrand can become singular or change very rapidly along the integration path, the range of integration is infinite and the integral may not be defined for some values of x and y. From the very nature of the Green function it is expected that the latter is the case at the source point and at the source point alone. Therefore the problems connected with the existence of the inversion integral appear in our case in the first layer only. Here the solution is split up into two parts: the Green function for the homogeneous half-space with the material properties of the first layer, which is a well known function [4] in the Fourier and in the space domains and into the remaining part, for which the inversion integral is well defined for all the values of x and y.

The displacement in the first layer is now given by:

$$w_1(x, y, \omega) = \overline{w}_1(x, y, \omega) - \frac{i}{2\mu_1} H_0^{(2)}((\omega/c_{s1})r) \tag{12}$$

where $r = (x^2 + y^2)^{1/2}$ and $H_0^{(2)}$ is Hankel's function of the zeroes order and of the second kind, which represents the contribution of the ray travelling from the

source to the receiver point without any reflection. Taking into account its integral representation [6] and the Fourier transform of the total displacement the Fourier transform of the remaining part of the displacement $\overline{W}_1(\xi, y, \omega)$ can be computed, for which the inversion integral exist and is bounded for all values of x and y. In the case of the one layer half-space problem we thus obtain:

$$\overline{W}_1(\xi, y, \omega) = \frac{\left(1 - \frac{\mu_H \gamma_H}{\mu_1 \gamma_1}\right) e^{\gamma_1 H_1} \cosh(\gamma_1 y)}{\mu_1 \gamma_1 \left[\sinh(\gamma_1 H_1) - \frac{\mu_H \gamma_H}{\mu_1 \gamma_1} \cosh(\gamma_1 H_1)\right]}. \tag{13}$$

Physically the expression above represents the contribution of the reflected waves to the displacement at the receiver point. The expressions for $\overline{W}_1(\xi, y, \omega)$ and $W_1(\xi, y, \omega)$ $i = 2, \ldots, n, H$, have from the point of the numeric Fourier inversion, some important features in common. The only singularities of the integrand are at the branch points defined with $\gamma_i = 0$; in the limit as $\xi \to \pm\infty$ they behave as $O\{\xi^{-1} \cdot \exp[-(2H_1 - y) \cdot |\xi|]\}$; the inversion integral is always bounded and for small values of x and y, which are common in soil strucutre interaction problems, their contribution to the total displacement is small.

The original Fourier inversion path runs through all the singularities of the integrand. For the purpose of numerical integration it is convenient to replace it by an equivalent one which is placed at a certain distance from the singularities. This can be achieved in our case only in two steps. First we introduce new the integration variable ζ which is defined as:

$$\zeta = (c_{sm}/\omega) \cdot \xi \tag{14}$$

where c_{sm} is the maximal shear wave velocity in any of the layers or the underlying half-space. In the new complex ζ plane the singularity closest to the imaginary ζ axis is at point (1.0, 0.0). Now an equivalent box shaped inversion path is selected,

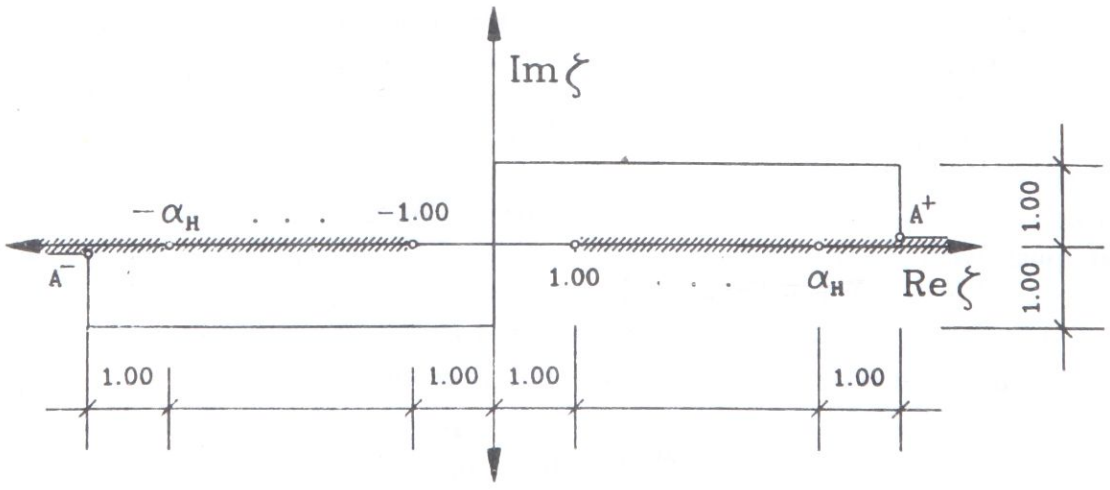

Fig. 3 The Fourier Inversion Paths and Integrals.

shown in Figure 3, in such a way that the smallest distance from it to any of the branch points is ≥ 1.0. Along it the transformed displacement varies slowly and the behavior of the inversion integrand is determined by its kernel only. The total integration path is now divided into seven intervals denoted in Figure 3 by I_1 to I_7. From the point of numerical integration they can be divided into three groups.

The integrals I_1 and I_7 are of semi infinite extent with the integrand, which behaves in an oscillatory way. It can be further seen that they are complex conjugates of one another and their sum is twice the real part of any one of them. The infinite range of integration can be reduced to a finite one by:

$$\begin{aligned} I_1 + I_7 = 2\,\mathrm{Re}\,I_7 &= \frac{c_{sm}}{\pi\omega}\,\mathrm{Re}\left(\int_{A+}^{\infty} W_i(\zeta, y, \omega) e^{-i(c_{sm}/\omega)\zeta x}\, d\zeta\right) \\ &= \frac{c_{sm}}{\pi\omega}\left[\cos\left(\frac{c_{sm}}{\omega} x A^+\right)\int_0^{(\pi\omega)/(c_{sm}x)} W_i^*(\zeta)\cos\left(\frac{c_{sm}}{\omega} x\zeta\right) d\zeta\right. \\ &\quad \left. - \sin\left(\frac{c_{sm}}{\omega} x A^+\right)\int_0^{(\pi\omega)/(c_{sm}x)} W_i^*(\zeta)\sin\left(\frac{c_{sm}}{\omega} x\zeta\right) d\zeta\right] \end{aligned} \tag{15}$$

where $W_i^*(\zeta)$ is defined as:

$$W_I^*(\zeta) = \sum_{k=0}^{\infty}(-1)^k W_i\left(\zeta + A^+ + k\frac{\pi\omega}{c_{sm}x}\right). \tag{16}$$

The integrals in Equation (15) can be evaluated by standard numerical procedures, therefore the infinite series in Equation (16) has to be computed. It has been shown that the transformed displacements $\overline{W}_1$ and W_i, $i = 2, ..., n, H$, decay rapidly with growing values of $|\zeta|$ and therefore the infinite series in Equation (16) converges very fast and only few terms are needed to obtain its sum with sufficient accuracy. After the evaluation of Equation (16) Romberg's procedure [5] has been adopted to compute the integrals in Equation (15).

The paths of the integrals I_3 and I_5 are parallel to the real ζ axis and of finite extent A^- to zero and zero to A^+ respectively. Along these paths the transformed displacements vary modestly with ζ, which is not the case with the kernel of the inverse Fourier transform, which for some values of the parameters x and ω oscillates rapidly. This could couse numerical instability if the usual formulas for numerical integration were applied. In our work it has been assumed that slowly varying transformed displacements can, with sufficient accuracy, be approximated by a quadratic parabola on a chosen interval. The integral I_k over such an interval then becomes:

$$I_k = \frac{1}{2\pi}\int_{-h+ci}^{h+ci} W_j(\zeta, y, \omega) e^{ig\zeta}\, d\zeta \approx \frac{1}{2\pi}\int_{-h}^{h} P_2(\zeta) e^{ig\zeta}\, d\zeta \tag{17}$$

where W_j denotes transformed displacements for $j = 2, ..., n, H$ and $\overline{W}_1$ if $j = 1$, c is ± 1, g is $-c_{sm}x/\omega$ and P_2 is polynomial of order two, which in the best possible way approximates W_j. After the coefficients of P_2 are expressed with the ordinates

of W_j the second integral in Equation (17) can be evaluated analytically. Thus we obtain:

$$I_k \approx \alpha(\theta)W_j(h,y,\omega)e^{\theta} + \beta(\theta)W_j(0,y,\omega) + \gamma(\theta)W_j(-h,y,\omega)e^{-\theta} \tag{18}$$

where $\theta = gh$ and

$$\begin{aligned} \alpha(\theta) = \bar{\gamma}(\theta) &= (h/2\theta^3)\left[(\theta - 2i)e^{-2i\theta} - 2i\theta^2 + 3\theta + 2i\right] \\ \beta(\theta) &= (4h/\theta^3)\left[\sin(\theta) - \theta\cos(\theta)\right]. \end{aligned} \tag{19}$$

The bar over γ denotes its complex conjugate. If high accuray of computation is required, a small h has to be chosen and θ becomes small too. In this case it is recommedable to replace Equations (19) by their power series expansions, which are given as:

$$\begin{aligned} \alpha(\theta) = \bar{\gamma}(\theta) &\approx \frac{h}{3} + \frac{h}{15}\theta^2 - \frac{2h}{105}\theta^4 + \cdots + i\left(-\frac{2h}{45}\theta^3 + \frac{2h}{315}\theta^5 - \cdots\right) \\ \beta(\theta) &\approx \frac{4h}{3} - \frac{2h}{15}\theta^2 + \frac{h}{210}\theta^4 - \cdots . \end{aligned} \tag{20}$$

The use of Equations (18) and (19) respectively (20) leaves the evaluation of integrals I_3 and I_5 unaffected by their oscillatory behavior and thus very stable and efficient.

The paths of the integrals I_2, I_4 and I_6 are parallel to the imaginary ζ axis. The behavior of the integrand along them is dominated by the kernel of the inverse Fourier transform, which in this case behaves exponentially. This does not lead to unstability of numerical computation, howerer it lowers its efficiency considerably. Therefore special integration formulas have been derived for this case, too. Their basic idea goes along the same lines as in the previous case, only the argument of the exponential function in now real not imaginary.

The above described techniques for the evaluation of integrals I_1 to I_7 are a very efficient tool in the wide range of low and medium frequencies ω and distances x for performing the inverse Fourier transform given in Equation (11). To demonstrate their use the example described in the following paragraph has been chosen.

5. Illustrative Example. As the illustrative example a half-space consisting of one layer on top of the underlying half-space has been chosen. To normalize it, the thickness of the layer, its shear modulus, and the shear wave velocity in it have been introduced as units. From them the nondimensional units for time and mass are derived. For the material properties in the underlying half-space the following nondimensional values have been adopted: shear modulus and shear wave velocity are equal 2.0. The nondimensional frequency of the driving forces is 1.0. For these parameters the values of the displacement along the surface of the half space have been computed and are presented in Figures 4 and 5. It could be immediately realized that the layered half space solution can be divided into three areas with respect to the x coordinate. In the vicinity of the source point the displacement of the surface is predominantly given by Hankel's function (Eq. 12) and the magnitude

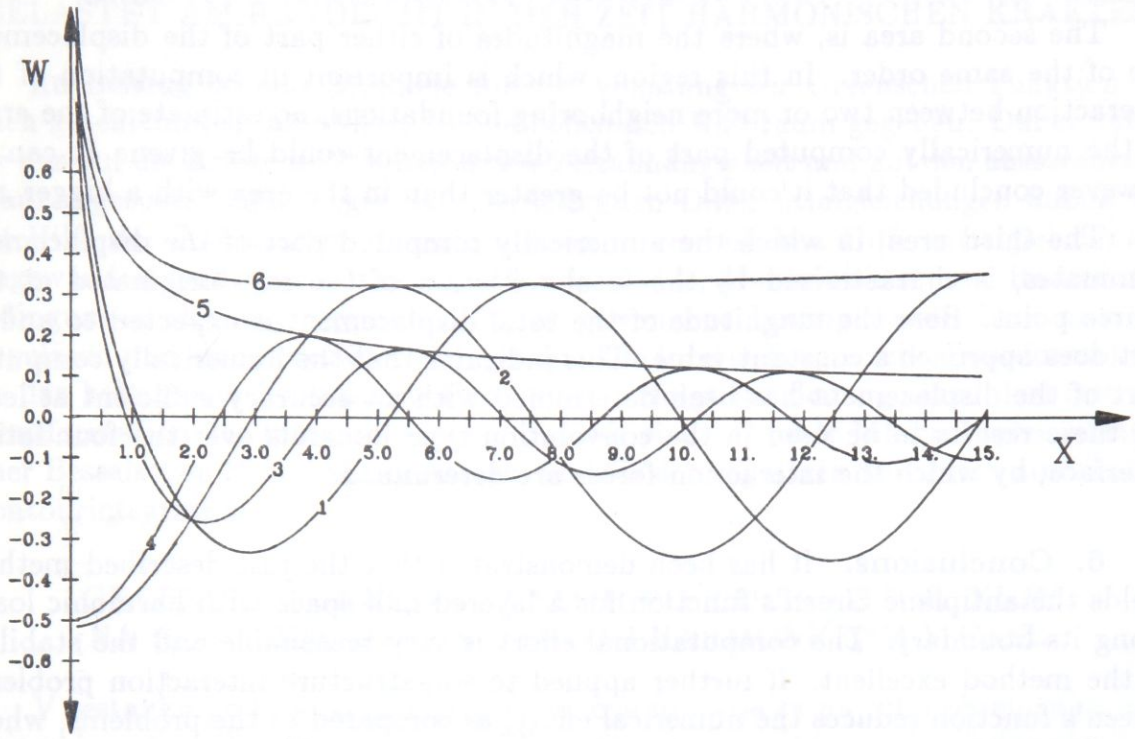

Fig. 4. Green's Function for the Illustrative Example: The real (1) and the imaginary part (4) of the regular part; the real (2) and the imaginary part (5) of the singular part; the real (3) and the imaginary part (6) of the total Green's function.

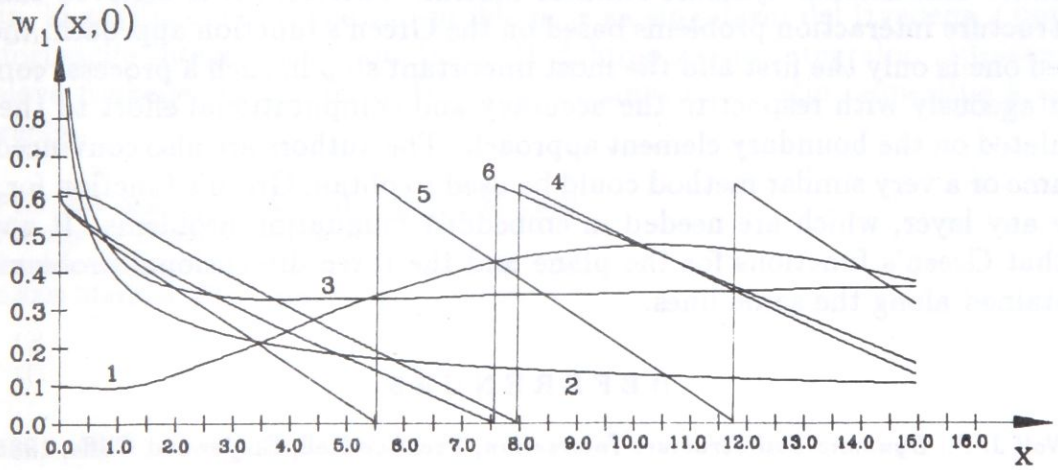

Fig. 5. Green's Function for the Illustrative Example: The absolute value (1) and the phase (4) of the regular part; the absolute value (2) and the phase (5) of the sangular part; the absolute value (3) and the phase (6) of the total Green's Function.

of the displacement $\bar{w}_1$ is for an order smaller. Since Hankel's function is through its polynomial approximation [6] known with extremely high accuracy, the relative smallness of the numerically computed part of the displacement guaranties by itself the highest quality of the results in this region. Since the width of a foundation is usually much smaller than the thickness of the layer, all the ordinates of Green's

function needed in soil structure interaction problems fall into this region.

The second area is, where the magnitudes of either part of the displacement are of the same order. In this region, which is important in computation of the interaction between two or more neighboring foundations, no estimate of the error of the numerically computed part of the displacement could be given. It can be however concluded that it could not be greater than in the area with a bigger x.

The third area, in which the numerically computed part of the displacement dominates, is characterized by the total reflection of the rays originated at the source point. Here the magnitude of the total displacement is expected to and in fact does approach a constant value. This indicates that the numerically computed part of the displacement has been determined with an accuracy sufficient at least for these results to be used in the convolution type integrals over the foundation interface, by which the interaction forces are determined.

6. Conclusions. It has been demonstrated that the just described method yields the antiplane Green's function for a layered half'space with harmonic loads along its boundary. The computational effort is very reasonable and the stability of the method excellent. If further applied to soil-structure interaction problems Green's function reduces the numerical effort, as compared to the problems, where a fundamental solution is used. The interaction integrals are to be defined along the soil structure interface only. So the problem is considerably reduced in size as compared to the use of fundamental solutions, where the integrals are to be defined along the surface of the half-space and along the layer interfaces leading to an infinite dimensional dynamic stiffness matrix. Therefore it is believed that the soil-structure interaction problems based on the Green's function approach, the just derived one is only the first and the most important step in such a process, compare advantageously with respect to the accuracy and computational effort to the ones formulated on the boundary element approach. The authors are also convinced that the same or a very similar method could be used to obtain Green's function for loads inside any layer, which are needed in embedded foundation problems. It appears also that Green's functions for the plane and the three dimensional problems can be obtained along the same lines.

REFERENCES

[1] Wolf J. P.: *Dynamic Soil-Structure Interaction*, Prentice-Hall, Englewood Cliffs, 1985.

[2] Kausel E.: *An Explicit Solution for the Green Function for the Dynamic Loads in Layered Media*, Research Report R81–13, Massachussetts Institute of Technology, 1981.

[3] Petyt M., Jones D. V.: *Effect of Layering on the Transmission of Ground Vibration*, in: Cakmak A. S. (ed.) Developments in Geotechnical Engineering Vol. **44**, Ground Motion and Engineering Seismology, Elsevier Computational Mechanics Publications, 1987.

[4] Achenbach J. D.: *Wave Propagation in Elastic Solids*, North-Holland, Amsterdam, 1975.

[5] Umek A., Štrukelj A.: *Dynamics of the Layered Half-Space*, ZAMM, Vol. **69**, No. 5, pp. 522–525, 1989.

[6] Abramowitz M., Stegun I. A. (ed.): *Handbook of Mathematical Functions*, Dover Publications, New York, 1968.

DIE GREENSCHE FUNKTION FUR EINEN GESCHICHTETEN HALBRAUM BELASTET AM RANDE MIT IN DER ZEIT HARMONISCHEN KRAFTEN

Im Beitrag ist eine Methode fur die Ableitung der Greenschen Funktion für einen geschichteten, an seinem Rande belasteten Halbraum gegeben. Dabei haben wir uns auf die Kräfte mit harmonischer Zeitabhängigkeit und auf den ausserebenen Spannungszustandsfall begrenzt. Die leitenden Differentialgleichungen haben wir mit Hilfe der Fourierschen Transformation in gewönlichen Differentialgleichungen umgewandelt und ihre Lösungen, die alle Rand-, Kontinuitäts- und Radiationsbedingungen erfüllen, bestimmt. Die so gewonnene Lösung wurde dann in einen singulären und einen regulären Teil geteilt. Die inverse Fouriersche Transformation, die das behandelte Problem zu Ende führt, erfolgt fur den sigulären Teil mit der Transformation des Integralweges so, daß wir eine bekannte Integralrepresentation einer Besselschen Funktion bekommen, und für den regulären Teil durch numerische Kontourintegration.

GREENOVA FUNKCIJA ZA SLOJEVIT POLPROSTOR, KI JE NA ROBU OBTEŽENEN Z SILAMI HARMONIČNIM V ČASU

V sestavku podajamo izpeljavo Greenove funkcije za na robu obremenjen slojevit polprostor. Pri tem smo se omejili na sile s harmonično časovno odvisnostjo in na izvenravninski slučaj. Vodilne diferencialne enačbe smo s pomočjo Fourierjeve transformacije prevedli v navadne diferencialne enačbe in določili njihove rešitve ob zadostatvi robnih, kontinuitetnih in radiacijskih pogojev. Tako dobljene rešitve smo razdelili v dva dela: singularnega in regularnega. Inverzna Fourierjeva transformacija, ki zaključuje obravnavani problem, je za singularni del izvedena s pomočjo transformacije integracijske poti tako, da dobimo znano integralno reprezentacijo Besselove funkcije, za regularni del pa jo izvršimo s pomočjo numerične konturne integracije.

Prof. dr. Andrej Umek & Mr. Andrej Štrukelj
Faculty of Technical Sciences
Smetanova 17,
62000 Maribor, POB 224